

Dispersity-Driven Melting Transition in Two-Dimensional Solids

M. Reza Sadr-Lahijany,¹ Purusattam Ray,^{1,2} and H. Eugene Stanley¹

¹*Center for Polymer Studies and Department of Physics, Boston University, Boston, Massachusetts 02215*

²*The Institute of Mathematical Sciences, CIT Campus, Chennai - 600 113, India*

(Received 19 May 1997)

We perform extensive simulations of 10^4 Lennard-Jones particles to study the effect of particle size dispersity on the thermodynamic stability of two-dimensional solids. We find a novel phase diagram in the dispersity-density parameter space. We observe that for large values of density there is a threshold value of the size dispersity above which the solid melts to a liquid along a line of first order phase transitions. For smaller values of density, our results are consistent with the presence of an intermediate hexatic phase. Further, these findings support the possibility of a multicritical point in the dispersity-density parameter space. [S0031-9007(97)04407-4]

PACS numbers: 64.70.Dv, 61.20.Ja, 64.60.Cn

Recently there has been considerable interest in what happens to the liquid-solid transition in a system if the constituent particles are not all identical but have different sizes. The question was first raised in the context of colloidal solutions [1], and subsequently addressed for other systems [2–5]. These studies focused mainly on the effect of size dispersity Δ on the P - ρ equation of state, where P and ρ denote pressure and density, respectively. On increasing Δ from zero, the density discontinuity at the transition decreases, eventually vanishing at a critical value $\Delta = \Delta_c$ above which there is no liquid-solid density discontinuity. This remarkable phenomenon—similar to the effect of temperature T on the conventional liquid-gas phase transition [6]—occurs in both two and three dimensions, and for various forms of interaction potentials and size distributions [4].

These seminal studies leave some questions unanswered. First, What are the structures of the phases? Second, Can one pass continuously from solid to liquid “around the critical point” at Δ_c , just as one can pass continuously from liquid to gas around the critical point at T_c ? A “yes” answer would not be consistent with the common picture of melting as a first order phase transition (which cannot have a critical point because of the symmetry mismatch of the two phases [7]). A “no” answer would lead to a natural third question: In the Δ - ρ parameter space, what is the location and nature of the phase boundary between crystalline and liquid phases? The third question has not gone unnoticed—indeed, Ref. [8] simulates a binary mixture of 108 “soft” disks, and shows that upon increasing Δ the crystal undergoes a transition to an amorphous solid at a threshold dispersity Δ_{th} , suggesting that the transition is of first order. In this Letter, we address all three questions. Our results suggest that, in the Δ - ρ parameter space, $C(\Delta_c, \rho_c)$ is a multicritical point at the junction of the liquid, solid, and hexatic phases. Above ρ_c , solid-to-liquid melting takes place through a first order phase transition, while below ρ_c the melting transition is continuous with the signature of an intermediate hexatic phase.

Our system is comprised of $N = 10^4$ Lennard-Jones particles of two different radii in a rectangular box of volume V and edges L_x and L_y , with periodic boundary condition. With each particle i , we associate a size parameter σ_i , and define the distance scale for the interaction between particles i and j to be $\sigma_{ij} \equiv \sigma_i + \sigma_j$. We assign to half of the particles the value $\sigma_i = \sigma_0(1 + \Delta)$, and to the other half the value $\sigma_i = \sigma_0(1 - \Delta)$. If particles i and j are at a distance r_{ij} smaller than a cutoff distance r_c , they interact via a “shifted-force Lennard-Jones” potential [9] $\Phi_{ij} = 4\epsilon[(\sigma_{ij}/r_{ij})^{12} - (\sigma_{ij}/r_{ij})^6] + f(r_{ij})$. Here $f(r_{ij})$ is a linear function whose coefficients are chosen such that Φ_{ij} and its gradient, the force, vanish continuously at $r_{ij} = r_c$. Since Φ_{ij} takes its minimum value at $r_{ij} = R_{ij} \equiv 2^{1/6} \times \sigma_{ij}$, we consider this equilibrium distance to be the sum of the radii of the two particles i and j , $R_{ij} = R_i + R_j$, so the radius of particle i is $R_i = 2^{1/6} \times \sigma_i$ and the average radius is $2^{1/6} \times \sigma_0$.

We perform molecular dynamics (MD) simulations using the velocity Verlet integrator method [9]. We record the results in reduced units in which σ_0 is 0.5, and the Lennard-Jones energy scale ϵ , the particle mass, and Boltzmann constant are all unity. In these units, we choose $r_c = 2.5$ and the length of each MD time step $\delta t = 0.01$. Using the Berendsen rescaling method [9], the system is first thermalized at $T = 1$ for a period of length τ , during which we make sure that it comes to equilibrium at T . Then we run the system for an additional period τ as a constant NVE system (microcanonical ensemble) where E is the total energy. We continuously calculate P, T , and E , the potential energy U and the total energy E , and we consider the system to be in equilibrium only when the fluctuations of all four quantities are less than 1% of their average values. The thermalization time τ is chosen to be more than the time it takes for the system to equilibrate. τ is typically $(5 \times 10^4)\delta t$ to $(2 \times 10^5)\delta t$.

We define the size dispersity by the ratio of the standard deviation to the average value of the size distribution [3], and this is Δ in our model. We define

$\rho \equiv \sum_{i=1}^N (\pi R_i^2) / (L_x \times L_y)$ as the ratio of the total area assigned to the disks to the system area. For each value of Δ , we start by placing the 10^4 particles randomly on the sites of a square lattice of edge $L_0 \approx 150$; higher density states are obtained by gradually compressing the system by reducing L_0 . Typically, the starting density is $\rho = 0.85$, and we increase ρ to 1.05 through approximately 10–20 intermediate densities, equilibrating the system at each [10]. For a few state points near the transition, we have checked our results for a rectangular lattice with aspect ratio $\sqrt{3}/2$ ($L_x = (\sqrt{3}/2)L_y$, with $L_x \times L_y \equiv L_0^2$) which accommodates a triangular lattice perfectly. This eliminates any possible artificial hindrance in crystallization arising from the asymmetry imposed by the shape of the square box.

We present our results for the state points with $T = 1$, $\rho = 0.90$ –1.05, and $\Delta = 0$ –0.12. At these densities, the $\Delta = 0$ system is a 2D solid with a triangular order, but at large Δ the system becomes disordered and a liquid. By probing the translational and orientational order, we determine the phase of each state point and we locate the transition between the two phases. To study translational order, we calculate the total pair correlation function $g(r)$, as well as the partial functions $g_{11}(r)$, $g_{22}(r)$ and $g_{12}(r)$ [9]. Here $g(r)$ is the probability distribution of finding two particles at a distance r , and $g_{ij}(r)$ is the same for an (i, j) pair ($i = 1$ stands for small and $i = 2$ for large particles). We find that all three $g_{ij}(r)$ display behavior similar to $g(r)$, indicating that the system maintains its substitutionally disordered configuration and does not tend toward de-mixing [11].

In Fig. 1(a) we show the effect of tuning Δ on translational order. We observe that the monodisperse ($\Delta = 0$) system shows the quasi-long-range translational order expected for a 2D solid [12], characterized by a power-law decay of the envelope of $g(r)$ and the persistence of the solid structure periodicity up to very large distances. For $\Delta < \Delta_{th}(\rho)$, where $\Delta_{th}(\rho)$ is the threshold value at fixed ρ , the solid maintains this quasi-

long-range order, although the decay exponent appears to increase somewhat with Δ . For $\Delta > \Delta_{th}(\rho)$, we observe a qualitative change in the structure: The quasi-long-range translational order disappears, and is replaced by an exponential decay of the envelope of $g(r)$, which at very long distances shows the uniform distribution of a structureless liquid. We observe this behavior for all densities between $\rho = 0.96$ and $\rho = 1.05$, and find that $0.09 < \Delta_{th}(\rho) < 0.10$ for all ρ .

Next we study the local bond orientational order by calculating for each particle j the sixfold orientational order parameter [13]

$$(\psi)_j \equiv \frac{1}{z} \sum_{k=0}^z e^{i6\theta_{jk}}. \quad (1)$$

The sum runs over all z nearest neighbors k of j , and θ_{jk} is the angle of the bond joining particles j and k with respect to a fixed axis. We identify the nearest neighbors as the particles that are closer than the location of the first minimum of $g(r)$. The modulus of $(\psi)_j$ will be unity if the neighbors form a perfect hexagon around j , which occurs for all particles in a triangular lattice, the close-packed configuration of a 2D solid. For a distorted hexagon or a different polygon, $|(\psi)_j| < 1$ —e.g., for a liquid, the distribution of $|(\psi)_j|$ centers around 0.5 [14].

We define the continuous order parameter field $\psi(\mathbf{r})$ as the value of $(\psi)_j$ if the position of particle j is $\mathbf{r}_j = \mathbf{r}$, and we calculate the orientational correlation function [15]

$$g_6(|\mathbf{r} - \mathbf{r}_0|) \equiv \langle \psi(\mathbf{r})\psi(\mathbf{r}_0) \rangle, \quad (2)$$

where $\langle \dots \rangle$ denotes an average over \mathbf{r}, \mathbf{r}_0 , and time. Figure 1(b) shows that, if Δ is small and ρ is large, the system displays the long-range orientational order of a solid in that $\lim_{r \rightarrow \infty} g_6(r) \neq 0$. Noteworthy is that, for each value of ρ , orientational order disappears upon a small increase in dispersity near $\Delta_{th}(\rho)$. For $\Delta > \Delta_{th}(\rho)$, $g_6(r)$ appears to decay exponentially, which identifies the system as a liquid. Most importantly, this change in the behavior of $g_6(r)$ is *abrupt* and *discontinuous* and takes place in a small range of Δ . Few runs within this range of Δ show either a solid phase or the liquid phase. We do not see the signature of any other phase with any power-law behavior. Similar plots for other large values of ρ suggest that, near $\rho = 1.0$, there is a first order phase transition from solid to liquid, driven by an increase in Δ . This observation is in agreement with the results of Ref. [8]. Figure 1 shows that the small dispersity system has the *ordered* structure of a solid while the large dispersity system has the *disordered* structure of a liquid—providing an answer to the first of the three questions.

Since identifying phases relies on the behavior of the system in the thermodynamic limit, we apply finite size scaling to the moments of the orientational order parameter ψ , which is the average value of $\psi(\mathbf{r})$. We use standard techniques originally developed for the Ising model [16], and recently applied to the 2D melting

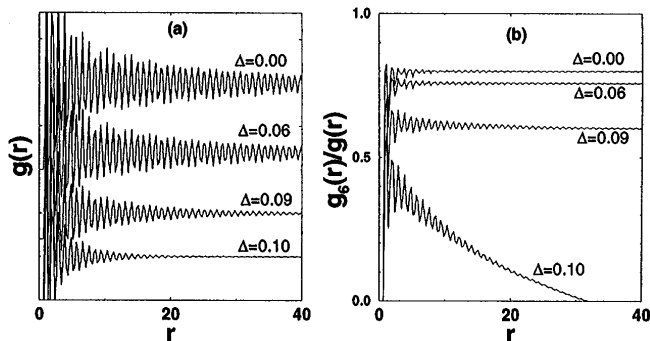


FIG. 1. Effect of Δ on translational and orientational order at $\rho = 1.0$. (a) Total pair correlation function $g(r)$ as a function of distance r . All curves oscillate around the value $g(r) = 1$, so we have separated them to facilitate comparison. (b) Normalized orientational correlation function versus r .

transition [17,18]. In order to calculate the moments of ψ at a scale $b \equiv L_0/M$, we divide the system into M^2 rectangular blocks of edges b_x and b_y ($b_x = L_x/M$, $b_y = L_y/M$) and we define ψ_b for each block as the absolute value of the average of $\psi(\mathbf{r})$ over the block. Then we find the moments of ψ_b by averaging over all blocks and all configurations of the system after equilibration.

To explore the precise location of the phase transition, we calculate the cumulant [17]

$$U_b \equiv 1 - \frac{\langle \psi_b^4 \rangle}{3\langle \psi_b^2 \rangle^2}. \quad (3)$$

For a completely *ordered* (solid) system, $U_b = 2/3$ in the thermodynamic limit while, for a *disordered* (liquid) system, $U_b \rightarrow 0$. For an infinite system, U_b jumps between these two limiting values at the phase transition point, and, for finite systems, this jump becomes rounded. Still, one can determine the location of a phase transition by finding the point at which the U_b curves for different system sizes intersect [17]. In Fig. 2, we plot U_b versus Δ , for different scales b at a fixed ρ . We find the transition from the value $2/3$ to lower values upon passing through the phase transition. Moreover, we estimate $\Delta_{th}(\rho)$ from the crossing point of the curves. In the phase diagram of Fig. 3, the line L_{th} is the locus of all such threshold points separating solid and liquid phases, and shows that, for $\rho > 0.96$, $\Delta_{th}(\rho) \approx 0.097$ is essentially independent of ρ .

Next we study the finite size scaling of $\langle \psi_b^2 \rangle$. Because of the qualitative difference in the form of $g_6(r)$ between solid and liquid, the behavior of $\langle \psi_b^2 \rangle$ as a function of b changes drastically upon melting [18]. In the *liquid* for $b \gg \xi$, where ξ is the correlation length, $\langle \psi_b^2 \rangle$ decays as b^{-2} , while for the *solid*, $\langle \psi_b^2 \rangle$ remains constant. Figure 4(a) shows that, for $\rho = 1.0$, the behavior of the system changes *abruptly* from solid (given by the line with zero slope) to liquid (slope -2) at Δ_{th} , which is con-

sistent with our previous studies of $g(r)$, $g_6(r)$, and U_b . The $\Delta = 0.10$ liquid curve shows a long-range correlation for $b < \xi$, which crosses over to a short-range correlation for $b \gg \xi$ ($\xi \approx 0.6L_0$ for this curve). The corresponding plots for larger Δ show that ξ shrinks upon increasing Δ . For $\rho = 0.9$ [Fig. 4(b)], we observe both solid behavior for $\Delta < 0.06$ and liquid behavior for $\Delta > 0.06$. For $\Delta = 0.06$, Fig. 4(b) shows an *algebraic* decay for the correlation function, with exponent $-1/4$. This “intermediate” behavior is reminiscent of the hexatic phase [18], for which the orientational correlation decays algebraically while the system does not possess quasi-long-range translational order. The locus of the points showing this intermediate behavior is shaded in Fig. 3.

In summary, we have studied a melting transition driven not by T but by Δ . We have simulated relatively large systems and applied finite size scaling (Figs. 2 and 4), arriving at a phase diagram for this dispersity-driven melting (Fig. 3). Melting takes place from a 2D ordered phase to a disordered liquid phase, similar to the conventional temperature-driven melting processes. Moreover, at large values of ρ , melting is a first order phase transition at a threshold dispersity value $\Delta_{th}(\rho) = 0.097 \pm 0.005$. Our study of the mean square displacement of the particles shows that this melting is accompanied by a transition from a frozen solid to a very slowly diffusive liquid, distinguishing it from the glass transition observed in [8] in the region studied, although the trend suggests the appearance of a glass at densities higher than $\rho = 1.05$. The threshold line L_{th} extends almost horizontally down to the point C with coordinates $\Delta_c \approx 0.097, \rho_c \approx 0.96$. Below ρ_c , finite size scaling of the orientational order parameter suggests the existence of an intermediate “hexatic” phase between the solid and liquid phases in the region of parameter space depicted in Fig. 3. Thus we hypothesize that point C is a multicritical point,

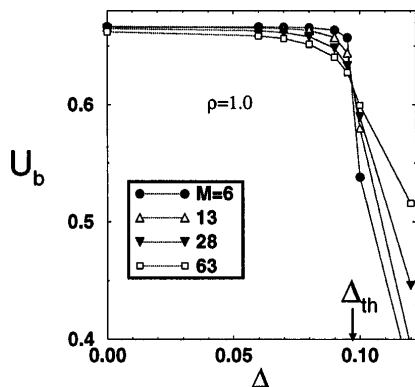


FIG. 2. Cumulant U_b of the bond orientational order parameter ψ as a function of dispersity Δ for $\rho = 1.0$. Different curves correspond to different scales b , where $b \equiv L_0/M$ is the block size, so smaller M corresponds to larger scale. The dotted lines connecting the data points are guides to the eye. We identify the threshold value of Δ to be the point where all the curves for different scales intersect.

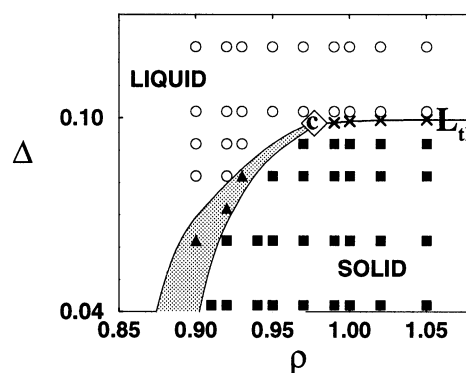


FIG. 3. Phase diagram in the Δ - ρ (dispersity-density) parameter space. Squares represent solid points and circles represent liquid points. The threshold line L_{th} connects the crosses, which are the first order phase transition points derived from the cumulant analysis. The triangles are the points of the intermediate phase (shaded), showing a hexatic behavior. The large diamond marks the multicritical point C .

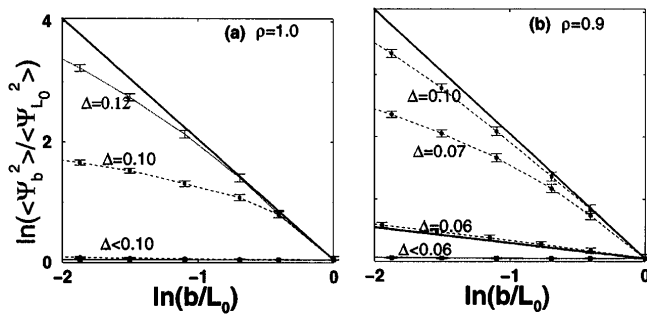


FIG. 4. Log-log plots of $\langle \psi_b^2 \rangle / \langle \psi_{L_0}^2 \rangle$ versus b for different dispersities Δ and for (a) $\rho = 1.0$ and (b) $\rho = 0.9$. Both axes are normalized by their values at system size L_0 , which causes the curves to meet at the origin and facilitates comparing their asymptotic slopes. The dashed lines connecting the data points are guides to the eye. The solid straight lines are reference lines with slopes -2 and $-1/4$.

where two lines of continuous transitions (separating liquid/hexatic and hexatic/solid phases) meet the line of first order transitions L_{th} (separating liquid/solid phases) as shown in Fig. 3 [19]. Figure 3 provides an answer to the last two of the three questions: one *cannot* pass continuously from solid to liquid around the critical point C , because the two phases are separated by the line of first order phase transitions L_{th} . Although our study is based on the bidisperse distribution of particle sizes, we believe our observations will be equally valid for other forms of distribution as well [4]. It is worth mentioning that a similar horizontal line of order-disorder transition has been observed in the study of the effect of quenched impurities on the structure of 2D solids [20].

We thank N. Ito for generously introducing us to this topic; S.T. Harrington for significant assistance in the formative stages of this research; J.L. Barrat for bringing Ref. [8] to our attention; L.A.N. Amaral, S.V. Buldyrev, N. Clark, W. Kob, B. Kutnjak-Urbanc, and D.R. Nelson for extremely helpful criticism; NSF and BP for financial support; and the Boston University Center for Computational Science for computational resources.

- [1] E. Dickinson, Chem. Phys. Lett. **57**, 148 (1978); J. Chem. Soc. Faraday Trans. 2 **75**, 466 (1979); E. Dickinson and R. Parker, Chem. Phys. Lett. **79**, 578 (1981); E. Dickinson, J. Phys. Lett. (Paris) **46**, L29 (1985).
- [2] J.L. Barrat and J.P. Hansen, J. Phys. (Paris) **47**, 1547 (1986).
- [3] P.N. Pusey, J. Phys. (Paris) **48**, 709 (1987).
- [4] W. Vermöhlen and N. Ito, Phys. Rev. E **51**, 4325 (1995); N. Ito, Int. J. Mod. Phys. C **7**, 275 (1996).
- [5] P.G. Bolhuis and D.A. Kofke, Phys. Rev. E **54**, 634 (1996).
- [6] Note that Δ is not a thermodynamic control parameter like T , but is a geometric parameter which changes the interaction Hamiltonian. In this respect, Δ is similar to bond or site concentration in a diluted Ising model, which

modifies the phase diagram and changes the position of the phase transition [see, e.g., A. Coniglio, Phys. Rev. Lett. **46**, 250 (1981)].

- [7] L.D. Landau and E.M. Lifshitz, *Statistical Physics*, translated by J.B. Sykes and M.J. Kearsley (Pergamon Press, New York, 1980), 3rd ed.; H.E. Stanley, *Introduction to Phase Transitions and Critical Phenomena* (Oxford University Press, New York, 1971).
- [8] L. Bocquet, J.P. Hansen, T. Biben, and P. Madden, J. Phys. Condens. Matter **4**, 2375 (1992).
- [9] M.P. Allen and D.J. Tildesley, *Computer Simulation of Liquids* (Oxford University Press, New York, 1989).
- [10] The average simulation speed on Boston University's SGI Origin2000 supercomputer was approximately $10 \mu s$ per particle update. So each of the state points studied here requires between 8 to 16 hours on one processor (over 10^3 hours total computational time).
- [11] For a few state points with large Δ and ρ values, we started with a phase separated configuration of the small and large disks. The runs which were continued up to 2 000 000 time steps at constant $T = 1$, show that the system goes toward complete mixing. This mixing is driven by entropy increase, which at the temperature studied seems to dominate the slight increase of U accompanying the order-disorder transition caused by mixing.
- [12] D.R. Nelson, in *Phase Transitions and Critical Phenomena*, edited by C. Domb and J.L. Lebowitz (Academic, London, 1983), Vol. 7.
- [13] D.R. Nelson and B.I. Halperin, Phys. Rev. B **21**, 5312 (1980).
- [14] M.A. Glaser and N.A. Clark, in *Geometry and Thermodynamics*, edited by J.C. Tolédano (Plenum, New York, 1990), p. 193; M.A. Glaser, N.A. Clark, A.J. Armstrong, and P.D. Beale, in *Dynamics and Patterns in Complex Fluids*, edited by A. Onuki and K. Kawasaki (Springer-Verlag, Berlin, 1990), p. 141.
- [15] D. Frenkel and J.P. McTague, Phys. Rev. Lett. **42**, 1632 (1979); J.P. McTague, D. Frenkel, and M.P. Allen, in *Ordering in Two Dimensions*, edited by S.K. Sinha (North-Holland, New York, 1980), p. 147.
- [16] K. Binder, Z. Phys. B **43**, 119 (1981).
- [17] H. Weber, D. Marx, and K. Binder, Phys. Rev. B **51**, 14 636 (1995).
- [18] K. Bagchi, H.C. Andersen, and W. Swope, Phys. Rev. Lett. **76**, 255 (1996); Phys. Rev. E **53**, 3794 (1996).
- [19] A similar phase diagram is observed for the temperature-driven melting transition in dislocation vector systems. The nature of the transition depends on the core energy E_c of the dislocations. At large E_c , melting takes place through the formation of the hexatic phase, whereas for small E_c the transition is predominantly first order. The resulting phase diagram in the $T-E_c$ parameter space is similar to our phase diagram in the $\Delta-\rho$ parameter space (Fig. 3), with the existence of a multicritical point at the junction of the liquid, hexatic and solid phases. [Y. Saito, Phys. Rev. Lett. **48**, 1114 (1982); Phys. Rev. B **26**, 6239 (1982)].
- [20] D.R. Nelson, Phys. Rev. B **27**, 2902 (1983); M.-C. Cha and H.A. Fertig, Phys. Rev. Lett. **74**, 4867 (1995).